Steel and Composite Structures, *Vol. 27, No. 5 (2018) 545-554*
DOI: https://doi.org/10.12989/scs.2018.27.5.545

Structural performance of cold-formed steel composite beams

M. Adil Dar [*1], N. Subramanian [2], M. Anbarasu [3], A.R. Dar [4] and James B.P. Lim [5]

[1] *Department of Civil Engineering, Indian Institute of Technology Delhi, New Delhi, India*
[2] *Consulting Engineer, Maryland, USA*
[3] *Department of Civil Engineering, Government College of Engineering Salem, Tamilnadu, India*
[4] *Department of Civil Engineering, National Institute of Technology Srinagar, J&K, India*
[5] *Department of Civil & Environmental Engineering, University of Auckland, New Zealand*

(*Received April 13, 2017, Revised February 8, 2018, Accepted April 23, 2018*)

Abstract. This study presents a novel method of improving the strength and stiffness of cold-formed steel (CFS) beams. Flexural members are primary members in most of the structures. Hence, there is an urgent need in the CFS industry to look beyond the conventional CFS beam sections and develop novel techniques to address the severe local buckling problems that exist in CFS flexural members. The primary objective of this study was to develop new CFS composite beam sections with improved structural performance and economy. This paper presents an experimental study conducted on different CFS composite beams with simply supported end conditions under four point loading. Material properties and geometric imperfections of the models were measured. The test strengths of the models are compared with the design strengths predicted by using Australian/New Zealand Standard for cold-formed steel structures. Furthermore, to ensure high precision testing, a special testing rig was also developed for testing of long span beams. The description of test models, testing rig features and test results are presented here. For better interpretation of results, a comparison of the test results with a hot rolled section is also presented. The test results have shown that the proposed CFS composite beams are promising both in terms of better structural performance as well as economy.

Keywords: failure modes; cold-formed steel composite beams; structural behavior; timber packing; critical load

1. Introduction

Structural safety, reliability and serviceability aspects require enhancement in the performance of CFS members, for large scale practical implementation, as they are potential light weight material. In contrast to hot rolling, where there is only a limited choice of cross sectional profiles, the cold-formed process, coupled with automatic welding, permits an unlimited variety of shapes, thus making this type of steel construction not only economical but also adoptable to special requirements (Zhao 2005, Yu and Schafer 2002, Dar *et al*. 2015a, Zhou and Jiang 2017). Furthermore, like other developing countries, structural designers in India, are faced with global competition in the design of fast track and cost effective structural systems to meet the huge deficit of various infrastructural systems. For this purpose, CFS sections provide an ideal choice not only for cost effective structural systems but also for the desired fast track construction (Siahaan *et al*. 2014, Wang and Young 2014c, Heva and Mahendran 2013, Anbarasu and Sukumar 2013, Kumar and Sahoo 2016, Zhou and Jiang 2017).

CFS sections, however suffer from some potential structural limitations, notable among them being their susceptibility to buckling when used as compression or flexural members (Lindner *et al*. 1983, Hancock 2001, Yu and Schafer 2002, Bayan *et al*. 2011, Anbarasu and Sukumar 2014). Hence there is a need to develop innovative techniques which will result in more efficient structural behaviour and also prove to be economical (Dar *et al*. 2015a, Tondini and Morbioli 2014). Such innovations include the development of efficient shapes and packing material/stiffening arrangement (Wang and Young 2014a). They result in economical use of material (i.e., high strength to weight ratio), potential for mass production, as well as ease in fabrication (i.e., allowing simple connection detailing to other structural members) (Wang and Young 2014b).

2. Previous work

Structural behavior of the commonly used CFS sections has been well researched in the past. However, only limited research has been undertaken to investigate the structural performance of new CFS composite beams. The history of developments on CFS flexural members can be traced back to 1965 when (O' Connor *et al*. 1965) first showed that the inclusion of various closed cells to I-section beams improved their performance against buckling failure significantly. They found that this improvement of buckling behaviour was mainly due to increase in torsional rigidity. This led the researchers to focus on CFS sections with torsionally rigid flanges, which can delay or eliminate structural instability problems effectively which being the

*Corresponding author, Senior Research Fellow,
E-mail: dar.adil89@gmail.com

ISSN: 1229-9367 (Print), 1598-6233 (Online)

main cause for the premature failure of such members at much lower loading. Zhao and Mahendran (2001) at Queensland University of Technology initiated a research program to investigate the structural behaviour and design of such torsionally rigid flange beam sections. Rectangular hollow flanges, from a single steel strip, were used by attaching them with spot welding, self-pierced riveting and screw fastening to form torsionally rigid flange beam sections. It was identified that the type of fastening and spacing does not affect the member compression capacity significantly. However, the structural behaviour and design of torsionally rigid flange beam as flexural members will be different. Hence it is important to identify the failure modes of torsionally rigid flange beams and develop suitable design rules for flexural members. Valse Ipe *et al*. (2013) investigated the role of shear connectors in developing the composite action in cold-formed steel composite beams. The novel simple bar type and conventional bolt type shear connectors in the shear zone of beams showed improved performance in composite beams both in terms of strength to weight ratio and ductility index. There was a good agreement between proposed analytical model and the experimental results. Hence analytical models based on rigid plastic theory developed were applicable for determining the flexural strength of cold-formed steel concrete composite beams. Laim *et al*. (2013) carried out a study on the structural behaviour of cold-formed steel beams with C-, I-, R- and 2R-shaped cross-sections. Four-point bending tests were carried out in order to assess mainly the failure loads and failure modes of the beams. It was observed that the failure loads of the beams with C- and lipped I-shaped cross-sections corresponded to the lateral torsional buckling modes, whereas the distortional buckling was the responsible buckling mode for the failure loads of the R and 2R beams. The use of two or more profiles in a beam can increase its strength-to-weight ratio. The 2R beams showed the best ratio. However, it seems that this ratio tends to be constant for beams comprised of more than four profiles. Lukowicz and Urbanska-Galewska (2014) developed new profile GEB that was also patented for the use for primary load-bearing member in fabricated steel frames. Extensive experimental study was carried out to investigate the feasibility of these new profiles. Paczos (2014) worked on the stability and limit load of cold-formed thin-walled channel beams with non-standard flanges subjected to pure bending. Critical and limit loads were obtained using a testing machine. Beams with box flanges lost stability before stresses exceeded the yield strength, but they collapsed in elastic–plastic and plastic range. There were some interactions between different types of buckling: web-flange interaction buckling, local–distortional buckling and flange local buckling. Further increase of load, after buckling, not only caused bigger deformation of cross-sections but also resulted in other buckling modes. Dar *et al*. (2015a) carried out research on various innovative CFS beam sectional profiles under flexure so as to find an ideal replacement for conventional hot-rolled steel sections, but would also be structurally very efficient and economical than the conventional cold-formed steel sections. The proposed sections successfully contributed towards delaying the various modes of premature buckling, enhancing load carrying capacity compared to common cold-formed steel sections.

The purpose of this paper is to investigate the feasibility of using high density expanded polystyrene and timber in CFS composite beams for improved strength and stiffness. Simply supported end conditions under four point loading are considered. The objectives of this study include proposing of different configurations of CFS beams using the composites, designing the CFS part of the composite beams using AS/NZS-4600, testing of proposed models using a 500 kN testing rig developed for high precision beam testing and testing of equivalent hot rolled steel beam for meaningful interpretation of results.

3. Statement of research

Stability failure, in the form of local bucking, is the main problem encountered in light gauge steel members. As discussed earlier, this local buckling failure occurs well before the material has reached its yield strength leaving the section under-utilized compared to its full capacity governed by strength failure. Hence it is desirable to develop CFS composite beams through new innovative sectional profiles and stiffening arrangements which would either delay or completely eliminate the local buckling failure thus allowing the section to reach its full load carrying capacity (Dar *et al*. 2015a, McDonald *et al*. 2008). It is well known that I- section profile is considered to be the most efficient under flexure. Thus to propose a replacement for the conventional I-section, some similar section has to be proposed. However, forming an I- section in light gauge steel by connecting two channel sections back to back (as is being generally done) will be susceptible to severe buckling, particularly in the compression zone. To overcome this limitation, there is a need to develop some novel composite CFS sections with a compression zone having adequate inherent resistance against such local buckling phenomena.

4. Justification for choosing proposed sections

Since the compression zone of the CFS beams is susceptible to severe buckling and torsion, it is necessary to develop such CFS composite beams whose compression zone will have the inherent resistance against local buckling. The following novel sections were proposed for the purpose.

4.1 Model A: Hollow box model

The sectional geometry of this model is also I shaped and consists of hollow rectangular box profile for both vulnerable zones, i.e., compression flange and web, as shown in Fig. 1. Only 1.6 mm thick sheet has been used for the fabrication of this model.

4.2 Model B: Box Model stiffened with high density expanded polystyrene packing

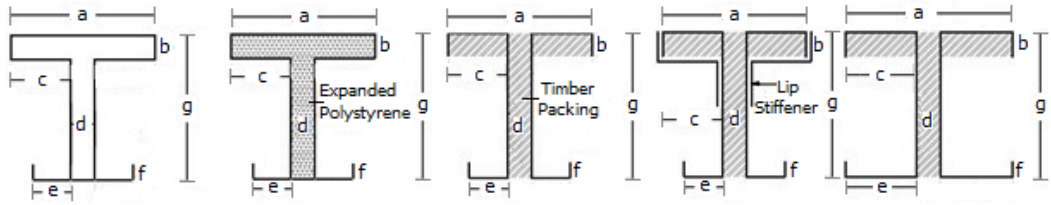

Fig. 1 Cross-Sectional details of all the models

Table 1 Model nominal and measured dimensions

Model	Nominal							Measured						
	a	b	c	d	e	f	g	a	b	c	d	e	f	g
A	150	25	62.5	25	40	15	150	148.2	24.8	62.0	24.6	38.8	14.1	149.1
B	150	25	62.5	25	40	15	150	149.5	24.6	61.8	24.0	39.2	14.5	148.7
C	150	25	62.5	25	40	15	150	148.4	24.3	62.3	23.9	39.5	14.4	148.2
D	150	25	62.5	25	40	15	150	149.4	24.6	62.3	24.5	39.5	14.8	149.0
E	150	25	62.5	25	40	15	150	149.0	23.9	62.0	24.5	39.8	14.3	149.3
F	150	25	75.0	25	75	25	150	174.6	24.0	74.7	24.5	74.2	24.7	149.7

Model B is modified version of Model A using specially ordered high density expanded polystyrene (density: 24 kg/m^3) packing as shown in Fig. 1 to investigate experimentally its contribution towards stiffening of vulnerable elements, particularly, compression flange against buckling as well as punching or bearing modes of failure under point loads. 1.6 mm thick sheet has only been used for fabrication of this model.

4.3 Model C: Box Model packed mainly with expanded polystyrene & locally with wooden pads under concentrated loads

After noticing localized punching mode of failure on compression side under concentrated loads during testing of Models A and B, it was expected that stiffer packing material like wood might arrest such a localized failure, thus greatly improving its structural performance. Accordingly, Model C, which is a modified version of Model B was fabricated replacing expanded polystyrene packing by wooden packing at locations of concentrated loads as shown in the Fig. 2. Rest of the details of Model C are kept strictly identical with Model B.

4.4 Model D: Timber stiffened model

Model D with unsymmetrical I shape (using two lipped channel sections back to back) involving simple fabrication was fabricated. The vulnerable elements, namely compression zone and web were stiffened by firmly attaching timber planks as shown in Fig. 1. Sufficient numbers of bolts were used to achieve the desired composite action. Only 1.6 mm thick sheet has been used for fabrication of this model.

4.5 Model E: Timber Stiffened Model with lip strengthening.

Having noticed localized lip failure of Model D in high *bending moment* zone, it was deemed necessary to improve its performance by strengthening lips against such failure. Accordingly, Model E which is a modified version of Model D was fabricated by strengthening the lips using steel strips of 1.6 mm as shown in Fig. 1 over the central zone of 1.5 m falling under higher *bending moment*.

4.6 Model F: Light weight timber stiffened model

Timber stiffened CFS composite beams (Models D and E) demonstrated higher strength and stiffness compared to the other ones. Hence research on similar beams was further continued on lighter CFS composite beams with similar stiffening arrangement with an objective to further increase the strength/weight ratio. Model F was fabricated consisting of symmetrical I shape using two lipped channel sections back to back and stiffened with timber planks as shown in Fig. 1. Sufficient bolts were used to achieve the desired composite action.1.2 mm thick sheet has only been used for fabrication of this model.

Dimensions of various elements of above referred models as indicated in Fig. 1 are given in Table 1.

4.7 Model G: ISMB-150.

One of the primary objectives of this study involves proposing of CFS composite beam section that can replace equivalent hot rolled beam. Therefore, a hot rolled beam serves as a benchmark model for the entire testing of models. Hence, hot rolled ISMB-150 @ 15kg/m, named Model G, was chosen as the reference beam model for testing as beam model (having all other conditions identical) to have meaningful comparison with experimental results of various CFS composite beams. Since Model G was a hot rolled steel beam, its load carrying capacity was determined by using Indian Standard (IS-800-2007).

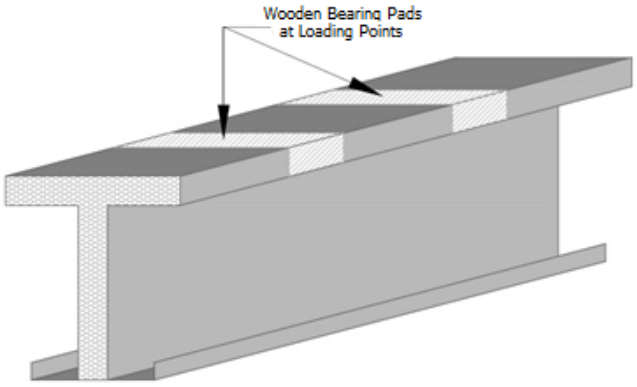

Fig. 2 Isometric view of Model C

Table 2 Material properties of steel used

Test	f_n	E (GPa)	f_y (MPa)	f_u (MPa)	Δ (%)
1	350	216	453	511	23%
2	350	205	467	495	19%
3	350	212	452	505	22%

5. Experimental program

5.1 Development of testing rig

For carrying out high precision testing on beam models, a 500 kN capacity Testing Rig as shown in Fig. 3(a), was developed to meet the requirements for high precision beam testing. Following are the salient features of the Testing Rig:

- A beam up-to a maximum of 7.5 m span, depth of 250 mm and width of 300 mm can be tested.
- A hydraulic jack of 500 kN capacity along with high precision 100 kN capacity proving ring.
- Suitable arrangement for application of four point loading as shown in Fig. 3(b). Load is applied through hydraulic jack on to the spreader beam as a single point load and is recorded. The load taken by the spreader beam is transferred to the model beam.
- The ideal steel framework which allows desired support conditions with inbuilt arrangement for the placement of dial gauges, and also allows easy mounting of beam models as shown in Fig. 3(a).

Table 3 Measured geometric imperfections at mid-length

Model	*A*	*B*	*C*	*D*	*E*	*F*
δ/L	1/2145	1/3123	1/254	1/4215	1/2126	1/3349

5.2 Material properties

Tensile coupon tests were used to determine the mechanical properties of steel used. Three coupons were prepared from the center of the flange in the longitudinal direction. Various standards exist which specify the requirements for testing of tensile specimens. However the dimensions of the coupons, as conforming to the Indian Standards (IS 1608 (2005)) were used for material testing. Computerized universal testing machine was used for conducting the tensile tests of the coupons. The relevant material properties of the steel obtained from the material testing are given in Table 2.

5.3 Geometric imperfections

Prior to testing, the initial overall geometric imperfections were measured. The imperfections were measured along the flange web junctions at the center. A theodolite was used to obtain the readings at the mid-length and near both ends of the models. The imperfections measured at the mid-length over the model is given in Table 3. The maximum geometric imperfection measured at the mid-length was 1/2126 of the Model E.

5.4 Constant characteristics of various Models

To achieve the various objectives of this research, six models with judiciously proposed specific variations in terms of sectional geometry and appropriate packing/ stiffening arrangements have been chosen for detailed experimental testing. To make the contribution of each specific improvement towards favourable structural performance prominently noticeable in experimental

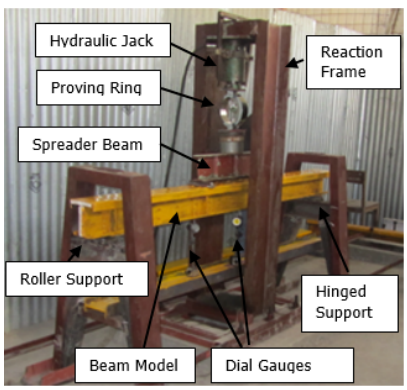

(a) Testing rig

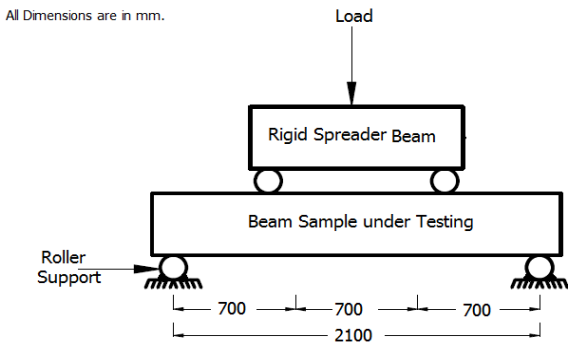

(b) Four point loading arrangement

Fig. 3 Experimental setup

testing, it was of paramount importance to ensure strict uniformity of various parameters which include span of the beam, support conditions, location of applied point loads and bearing/stiffening arrangement under concentrated applied load/reaction points (Dar *et al*. 2015b).

6. Test results and discussion

Sometimes semi-log curves are plotted for better interpretation of results (Manikandan *et al*. 2014). The log of load versus deflection curves along with corresponding modes of failure for various models are described below.

Fig. 4(a) shows the load versus mid span deflection curve of Model A. The model experienced premature local buckling failure in the box compression flange under bearing pads at applied concentrated loading points (apparently looking like punching failure) as is clearly seen in Fig. 4(b). The failure occurred at a critical load of 25.6 kN with corresponding displacement of 12.38 mm. The main reason for such a failure was due to non-continuity of bearing stiffeners. Except for a localized buckling failure on top face of box compression flange confined to very small length, rest of the model was found in sound condition and still possessing enough reserve strength.

Fig. 5(a) shows the load versus mid-span deflection curve of Model B. In addition to the similar mode of failure as observed in Model A, the Model B experienced premature localized failure in the web under/adjacent to the concentrated loading points as seen in Fig. 5(b). This failure was also accompanied by localized lip buckling at the same location as seen in Fig. 5(c) (an upper view of the compression flange when viewed from downside). The failure modes were noticed corresponding to a critical load of 27.3 kN with mid span displacement of 4.96 mm. In spite of its high density quality (specially ordered for this purpose), the expanded polystyrene packing to act as effective stiffening arrangement (against premature buckling modes of failure) did not prove to be successful as expected. Hence, it was not adopted in further test models.

Except localized buckling failure especially on top face of box compression flange, in both models A and B, restricted to very small length, rest of the Model B was found in sound condition and still possessing enough reserve strength. After noticing mainly localized punching mode of failure on compression side under concentrated loads in these models, it was expected that stiffer packing material like wood at the vulnerable locations may help in arresting such localized buckling failure which would thus greatly improve the structural performance.

Fig. 6(a) shows the load versus mid-span deflection curve of Model C. Unlike models A & B, the Model C continued to offer resistance to a higher loading. The model experienced multiple buckling failure modes particularly, localized web buckling under concentrated applied loads as seen in Fig. 6(c) (an upper view of the compression flange when viewed from downside). This was further followed by web buckling away from bolt line near applied load point as

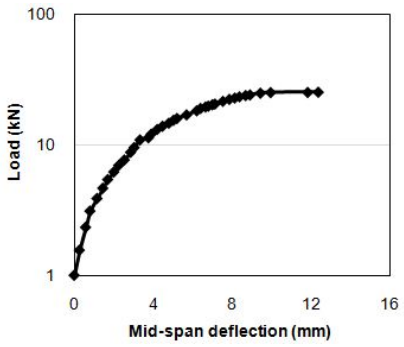

(a) Load displacement curve for Model A

(b) Compression flange buckling in Model A

Fig. 4 Test results for Model A

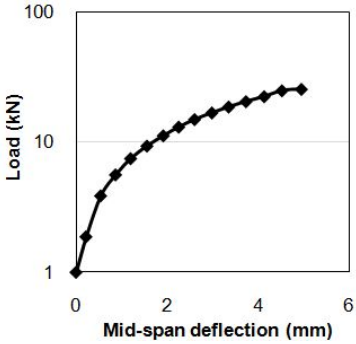

(a) Load displacement curve for Model B

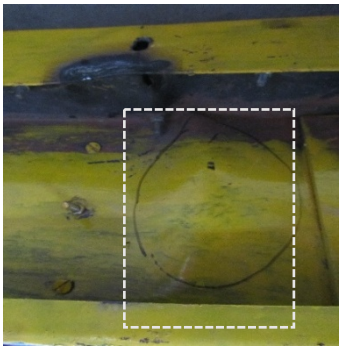

(b) Web buckling in Model B

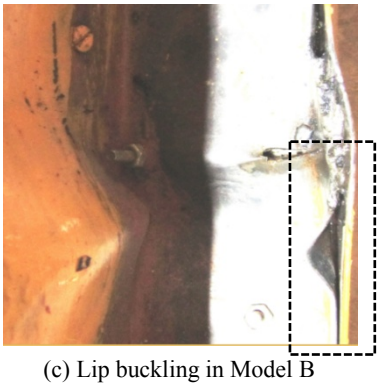

(c) Lip buckling in Model B

Fig. 5 Test results for Model B

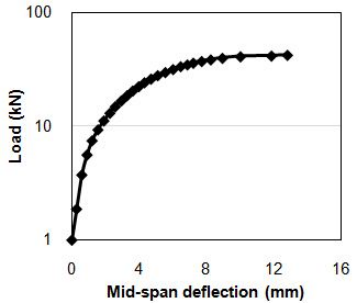

(a) Load displacement curve for Model C

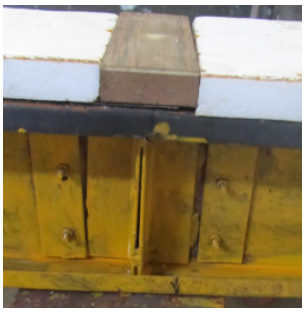

(b) Wooden bearing under loading points in Model C

(c) Web buckling in Model C

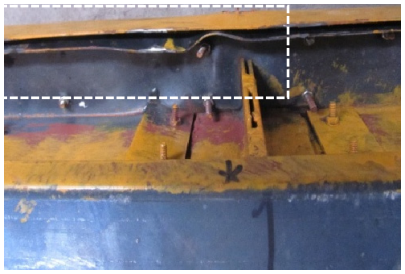

(d) Lip buckling in Model C

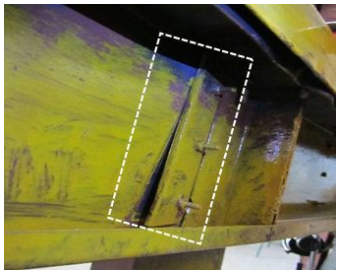

(e) Inadequate width of bearing stiffener in Model C

Fig. 6 Test results for Model C

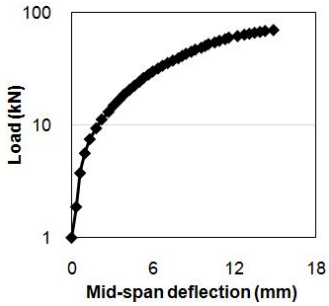

(a) Load displacement curve for Model D

(b) Lip buckling in Model D

(c) Flange buckling in Model D

Fig. 7 Test results for Model D

seen in Fig. 6(e) which finally culminated through lip buckling within high bending moment zone as is clear from Fig. 6(d). The extra resistance offered by the beam was partly due to reserve capacity of the section and partly due to strain hardening. It is worth highlighting here that the stiffening measures adopted through replacement of expanded polystyrene by wooden pads locally at vulnerable spots (i.e., under concentrated applied load points) as shown in Fig. 6(b) has greatly contributed to much improved load carrying capacity from 25.6 kN to 42.5 kN (i.e., an increase of 66% in load carrying capacity). Further, the localized failure got transformed into overall failure spread over larger length within high compressive stress. This encouraging experimental result confirms the important role of judiciously provided stiffening arrangements in improved performance of CFS construction.

The unstiffened zones between the adjacent appropriate timber stiffened zones became vulnerable spots to undesirable buckling modes of failure. To avoid such a vulnerability, it was deemed appropriate to replace expanded polystyrene with timber completely and was according followed in Model D.

Further to avoid buckling of web adjacent to angle stiffeners as seen in Fig. 6(e) due to inadequate bolted connection of web with stiffeners, it would be appropriate to strengthen the bolted connection further with welded connection along the toe of the stiffening angle.

Fig. 7(a) shows the load versus mid-span deflection curve of Model D. The model experienced premature localized buckling failure in the lip within the max bending moment zone and closer to the applied concentrated load on the left side prominently noticeable as seen in Fig. 7(b). The model could resist load up 70 kN with the corresponding mid span displacement of 16.08 mm. At this stage, the model suddenly stopped resisting any further load, hence considered as the critical load of Model D. This failure was accompanied by slight flange buckling at the same location as seen in Fig. 7(c). It needs to be highlighted here that unlike expanded polystyrene packing, the timber planks firmly connected to this model by simple fabrication has

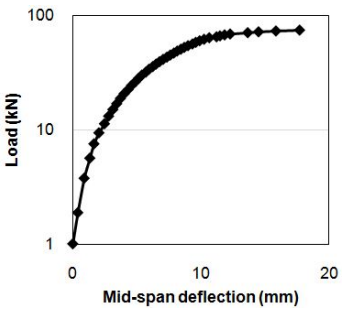

(a) Load displacement curve for model E

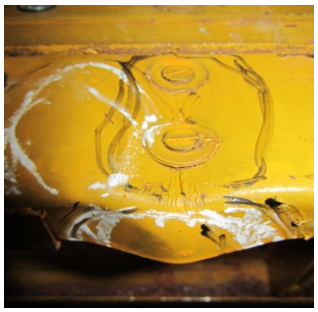

(b) Lip buckling in Model E

(c) Flange buckling in Model E

Fig. 8 Test results for Model E

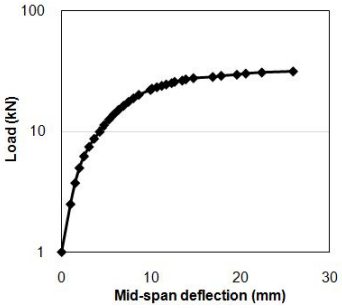

(a) Load displacement curve for Model F

(b) Flange buckling in Model F

(c) Lip buckling in Model F

(d) Compression flange failure in Model F

Fig. 9 Test results for Model F

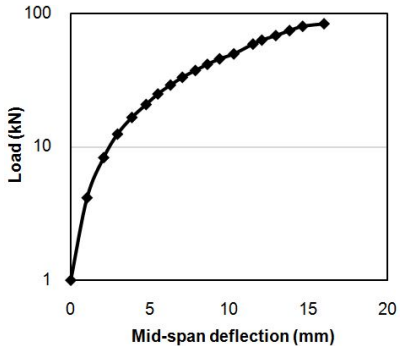

(a) Load displacement curve for Model G

(b) Lateral buckling mode in Model G

Fig. 10 Test results for Model G

drastically improved the load carrying capacity from 42.5 kN to 70 kN (i.e., an increase of 70% in the load carrying capacity). Except localized lip buckling, the flange failure was confined to a very small length; rest of the model apparently was in good condition and might have some reserve strength.

To utilize the expected reserved strength, it was deemed appropriate to modify Model D by strengthening the weakened spot and at similar vulnerable locations. Accordingly necessary modifications were made and appropriate strengthening measures were also taken by providing lateral intermittent stiffeners at the failure spot and other similar locations. The modified model was named as Model E.

Fig. 8(a) shows the load versus mid-span deflection curve of the Model E. This modified model (Model E) failed at a critical load of 74.4 kN against 70 kN resisted by Model D, which was much lower than expected. The pattern of failure observed was again local lip buckling followed by compression flange buckling, both near left support as seen in Figs. 8(b) and (c).

Fig. 9(a) shows the load versus mid-span deflection curve of Model F. The beam continued to resist higher load, partly due to reserve capacity of the section and partly due to strain hardening. The model failed at a critical load of 31.25 kN with a deflection of 25.9 mm at the centre. Localized lip buckling failure followed by buckling of compression zone were observed near one of the applied loading points as seen in Figs. 9(b), (c) and (d).

Fig. 10(a) shows the load versus mid-span deflection

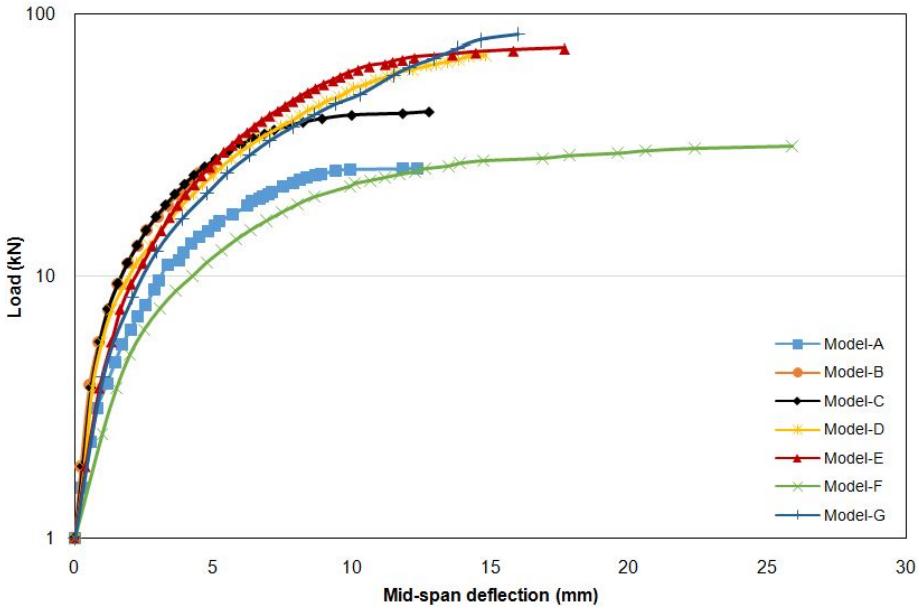

Fig. 11 Comparison of the various models

Table 4 Summary of test results

Models	W (kg/m)	Z (10^4 mm^3)	$P_{AS/NZS\ 4600}$ (kN)	P_{Exp} (kN)	$P_{Exp}/P_{AS/NZS\ 4600}$	M (kN-m)	δ (mm)	P_{Exp}/W	Mode of failure
A	19.80	6.60	30.4	25.63	0.84	08.96	12.38	1.29	FB
B	19.80	6.60	30.4	27.30	0.89	09.55	04.96	1.38	WB+LB
C	19.80	6.60	30.4	42.50	1.40	14.87	14.64	2.14	WB+LB
D	18.44	69.0	28.2	70.00	2.48	24.50	16.08	3.79	LB+FB
E	18.44	69.0	28.2	74.38	2.64	26.03	17.70	4.03	LB+FB
F	13.77	37.3	18.7	31.25	1.67	10.93	25.90	1.67	LB+FB
Age.	1.65								
S.D.	0.70								
G	32.00	1.10	65.7*	83.65	1.27	29.27	16.20	2.58	Lt. B

* The load carrying capacity of Model G was determined by using Indian Standard (IS-800-2007)

curve of Model G. The model experienced lateral buckling as seen in Fig. 10(b) corresponding to critical load of 83.65 kN and mid-span deflection of 16 mm.

The summary of the test results of all the models is given in Table 4 and their comparison in graphical form is depicted in Fig. 11.

7. Conclusions

The present study was able to successfully test and validate the feasibility of using expanded polystyrene and timber in various CFS composite beams through experimental testing. The prominent results obtained in this study are highlighted as under:

- Initially a low cost innovative stiffening arrangement against premature buckling was attempted using high density expanded polystyrene as packing to fill the hollow space within the proposed innovative box compression flange. However, the local buckling failure on top face of box compression flange was observed at much lower load thus failed to produce expected results.
- Replacement of softer expanded polystyrene by wooden pads, at vulnerable spots (i.e., under concentrated applied load points), results in to much improved load carrying capacity from 27.3 kN (Model B) to 42.5 kN (Model C) (i.e., increase in strength by 55%). This confirms the importance of proper application of stiffening arrangements in CFS composite beam sections.
- The improved model (i.e., Model D) using timber planks throughout firmly connected to the conventional cold form lipped I section (in order to facilitate much easy fabrication) drastically improved the load carrying capacity from 42.5 kN (Model C)to 70 kN (Model D) (i.e., increase in

strength by 64.7%). The strength / weight ratio of the timber stiffened model (i.e., 4.03) is considerably higher than that of hot rolled beam (i.e., 2.58) (i.e., 56.2%), thus proving the economy and better structural performance of the proposed stiffening system.

- It was also observed that the lighter CFS beam model (Model F) with timber stiffening can produce promising results when the section has adequate wall thickness i.e., not less than 1.5 mm.
- The lip strengthening of Model E in the high bending moment zone did not prove favourable as improvement in the strength was found out to be just 6.25%.
- Lip buckling, flange buckling and web buckling were the primary types of failure observed.
- The minimum and maximum geometric imperfections observed at mid-lengths in the various models were 1/4215 mm and 1/2126 mm respectively.
- It was found out that the design strengths predicted by AS/NZS-4600 are conservative for all models except Model A and B. It is because the consideration of material defects and other uncertainties can cause great reduction on the design strength. The minimum and maximum ratio of $P_{Exp}/P_{AS/NZS\ 4600}$ was found out to be 0.84 and 2.64 respectively. The test results in Models C to F were higher than the predicted design strengths as per AS/NZS 4600. This was mainly due to the composite action between cold-formed steel and timber in these models.

Acknowledgments

The experimental work described in this paper has been supported by a grant from Consulting Engineers, PVT. LTD (Project No. CES2015/8360). The authors would like to thank the Civil Engineering Department of National Institute of Technology Srinagar for their support by permitting the testing of the models in their Structural Engineering Laboratory. Prior to joining IIT Delhi, M. Adil Dar was working as an M.Tech. scholar in Structural engineering at Kurukshetra University and wishes to thank the University for their support. The authors also wish to thank the anonymous Reviewers for their valuable and constructive comments.

References

Anbarasu, M. and Sukumar, S. (2013), "Study on the effect of ties in the intermediate length cold formed steel (CFS) columns", *Struct. Eng. Mech., Int. J.*, **46**(3), 323-335.

Anbarasu, M. and Sukumar, S, (2014), "Influence of spacers on ultimate strength of intermediate length thin walled columns", *Steel Compos. Struct., Int. J.*, **16**(4), 37-454.

Bayan, A, Sariffuddin, S. and Hanim, O. (2011), "Cold-formed steel joints and structures -A review", *Int. J. Civil Struct. Eng.*, **2**(2), 621-634.

Dar, M.A., Yusuf, M., Dar, A.R. and Raju, J. (2015), "Experimental study on innovative sections for cold formed steel beams", *Steel Compos. Struct., Int. J.*, **19**(6), 1599-1610.

Dar, M.A., Subramanian, N., Dar, A.R. and Raju, J. (2015), "Experimental investigations on the structural behaviour of a distressed bridge", *Struct. Eng. Mech., Int. J.*, **56**(4), 695-705.

Dubina, D., Ungureanu, V. and Landolfo, R. (2012), Design of Cold-formed Steel Structures: Eurocode 3: Design of Steel Structures. Part 1-3 Design of cold-formed Steel Structures, Wiley.

Hancock, G.M. (2001), *Cold-Formed Steel Designing and Analysis*, Marcel Dekker, Sydney, Australia.

Heva, Y.B. and Mahendran, M. (2013), "Flexural-torsional buckling tests of cold-formed steel compression members at elevated temperatures", *Steel Compos. Struct., Int. J.*, 14(3), 205-227.

IS 1608 (2005), Indian Standard- Metallic Materials - Tensile Testing at Ambient Temperature; Bureau of Indian Standards, New Delhi, India.

IS 800 (2007), Indian Standard Code of Practice for General Construction in Steel; Bureau of Indian Standards, New Delhi, India.

Kumar, N. and Sahoo, D.R. (2016), "Optimization of lip length and aspect ratio of thin channel sections under minor axes bending", *Thin-Wall. Struct.*, **100**, 158-169.

Laim, L., Rodrigues, J.P.C. and da Silva, L.S. (2013), "Experimental and numerical analysis on the structural behaviour of cold-formed steel beams", *Thin-Wall. Struct.*, **72**, 1-13.

Lindner, J., Schmidt, J.S. and Subramanian, N. (1983), "Traglastversuche an zweifeldtragern mit dunnwandigen C-Profilen", Der Stahlbau, Volume 52, May, pp. 143-147.

Lukowicz, A. and Urbanska-Galewska, E. (2014), "Deformations of innovative cold-formed 'GEB' sections", *Proceedings of the 7th European Conference on Steel and Composite Structures*, Naples, Italy, September.

Manikandan, P., Sukumar, S. and Balaji, T.U. (2014), "Effective shaping of cold-formed thin-walled built-up beams in pure bending", *Arab. J. Sci. Eng.*, **39**(8), 6043-6054.

McDonald, M., Heiyantuduwa, M.A. and Rhodes, J. (2008), "Recent developments in the design of cold-formed steel members and structures", *Thin-Wall. Struct.*, **46**(9), 1047-1053.

O'Connor, C., Goldsmith, P.R. and Ryall, T.J. (1965), "The Reinforcement of Steel Beams to improve Beam Buckling Strength", Civil Engineering Transaction, Institute of Engineers Australia.

Paczos, P. (2014), "Experimental investigation of C-beams with non-standard flanges", *J. Constr. Steel Res.*, **93**, 77-87.

Siahaan, R., Keerthan, P. and Mahendran, M. (2014), "Section moment capacity tests of rivet-fastened rectangular hollow flange channel beams", *Proceedings of the 22nd International Specialty Conference on Cold-Formed Steel Design and Construction*, St. Louis, MO, USA, November, pp. 277-294.

Standards of Australia (2005), Cold-formed Steel Structures, AS/NZS 4600.

Tondini, N. and Morbioli, A. (2014), "Experimental analysis of cold-formed steel rectangular hollow flange sections", *Proceedings of European Conference on Steel and Composite Structures*, Naples, Italy, September.

Valsa Ipe, T., Sharada Bai, H., Manjulavani, K. and Iqbal, M.M.Z. (2013), "Flexural behaviour of cold-formed steel-concrete composite beams", *Steel Compos. Struct., Int. J.*, **14**(2), 105-120.

Wang, L. and Young, B. (2014a), "Cold-formed steel channel sections with web stiffeners subjected to local and distortional buckling – Part I: tests and finite element analysis", *Proceedings of the 22nd International Specialty Conference on Cold-Formed Steel Design and Construction*, St. Louis, MO, USA,

November, pp. 229-242.
Wang, L. and Young, B. (2014b), "Cold-formed steel channel sections with web stiffeners subjected to local and distortional buckling – Part II: parametric study and design rules", *Proceedings of the 22nd International Specialty Conference on Cold-Formed Steel Design and Construction*, St. Louis, MO, USA, November, pp. 243-258.
Wang, L. and Young, B. (2014c), "Design of cold-formed steel channels with stiffened webs subjected to bending", *Thin-Wall. Struct*., **85**, 81-92.
Wang, F.L., Yang, J. and Lim, J. (2014), "Numerical studies of collapse behaviour of multi-span beams with cold-formed sigma sections', In *Proceedings of the 22nd International Specialty Conference on Cold-Formed Steel Design and Construction*, St. Louis, MO, USA, November, pp. 345-358.
Winter, G. (1970), *Commentary on the 1968 Edition of the specification for the Design of Cold-formed Steel Structural Members*, American Iron & Steel Institute, New York, NY, USA.
Yu, C. and Schafer, B.W. (2002), "Local buckling tests on cold-formed steel beams", *Proceedings of the 16th International Specialty Conference on Cold- Formed Steel Structures*, Orlando, FL, USA, October.
Yu, C. and Schafer, B.W. (2006), "Distortional buckling tests on cold-formed steel beams", *J. Struct. Eng., ASCE*, **132**(4), 515-528.
Zhao, W. (2001), "Behaviour and design of cold-formed steel hollow flange sections under axial compression", Ph.D. Thesis; School of Civil Engineering, Queensland University of Technology, Brisbane, Australia.
Zhou, W. and Jiang, L. (2017), "Distortional buckling of cold-formed lipped channel columns subjected to axial compression", *Steel Compos. Struct., Int. J.*, **23**(3), 331-338.

CC

Nomenclature

a	Width of top compression flange
b	Depth of compression flange lip
c	Width of bottom compression flange
D	Spacing between web plates
e	Width of tension flange
f	Depth of tension flange lip
g	Depth of the section
f_n	Nominal yield strength
f_y	Yield strength
f_u	Ultimate strength
E	Modulus of Elasticity
Δ	Elongation (tensile strain) after fracture based on gauge length of 50 mm
W	Weight of the beam model
Z	Section modulus
$P_{AS/NZS\ 4600}$	Design strength predicted by AS/NZS 4600
P_{Exp}	Test strength
M	Moment in the central mid-third portion
δ	Deflection at the mid-span
LB	Lip buckling
FB	Flange buckling
WB	Web buckling
Lt. B	Lateral buckling
CFS	Cold-formed steel
Ave	Average
S.D.	Standard deviation